Swedish Hydroclimatic Data 1961-2020 – Precipitation, Temperature and Streamflow Observations across 50 Catchments (CAMELS-SE)

Creator: Claudia Teutschbein, Department of Earth Sciences, Uppsala University

Dataset correspondence: claudia.teutschbein@geo.uu.se

Publication year: 2024

Description: The hydroclimatic dataset for Sweden spans six decades and encompasses daily observations of hydroclimatic variables across 50 catchments in Sweden, including precipitation, temperature, and streamflow, enriched with valuable information about the geographical characteristics, land cover, soil classes, and regulation statuses for each catchment. Additionally, this dataset includes a comprehensive array of hydrological signatures that effectively capture the behavioral functions exhibited by each catchment. Importantly, this dataset is made accessible to an international audience, contributing a new region to the collection of existing CAMELS (Catchment Attributes and MEteorology for Large-sample Studies) datasets and facilitating transdisciplinary research with potential use cases outlined further below.

1. Data Description and development

1.1. Catchment Description

The data set comprises 50 Swedish catchments with distinct physiographic and hydroclimatic features (Table 1), varying in their upstream areas (2 km² to 8,425 km²) and covering a latitudinal gradient from 56°N to 68°N. Among these, 10 catchments fall under the category of transboundary, with more than 5% of their total area extending into Norway.

Table 1. Summary of hydroclimatic and catchment properties of the 50 catchments

Catchment Properties		Mean	Median	Min - Max
(1) Geographic properties	Latitude [°N, WGS84]	61.2	60.5	55.9 - 68.4
	Catchment area [km²]	1,404	1,012	2 - 8,425
	Mean elevation [m a.s.l.]	360	255	12 - 942
(2) Land cover	Agriculture [%]	10	2	0 - 100
	Forest [%]	55	62	0 - 86
	Glaciers [%]	0	0	0 - 2
	Open land [%]	3	0	0 - 38
	Shrubs and grassland [%]	16	11	0 - 77
	Urban [%]	1	0	0 - 3
	Water, i.e., streams and lakes [%]	6	5	0 - 16
	Wetlands [%]	8	4	0 - 33
(3) Soil types	Bedrock and glaciers [%]	17	10	0 - 70
	Clayey till and clay till [%]	0	0	0 - 7
	Glaciofluvial sediments [%]	7	6	0 - 29
	Peat [%]	8	6	0 - 35
	Postglacial sand-gravel [%]	2	0	0 - 18
	Silt [%]	3	0	0 - 25
	Till [%]	47	50	0 - 98
	Till and weathered deposit [%]	6	0	0 - 57
(4) Hydroclimatic properties	Mean annual temperature [°C]	3.3	2.8	-2.8 - +7.9
	Mean annual precipitation [mm year^{-1}]	803	767	544 - 1,196
	Mean annual streamflow [mm year^{-1}]	481	378	168 - 1,312

Encompassing all three major climate zones in Sweden (Figure 1a), the 50 catchments include the polar tundra climate zone in the Scandinavian Mountains, the subarctic boreal climate in central and northern Sweden, and the warm-summer hemiboreal climate zone in the south. Most of the catchments have a predominantly humid climate, with an average annual precipitation of 803 mm during the period 1961-2020. Notably, the western parts of Sweden experience the highest precipitation rates (Figure 1b).

In this collection of catchments, those dominated by snowmelt and those in transitional states outnumber rain-dominated ones. Moreover, nearly half of the catchments receive over a third of their total annual precipitation as snowfall. During the period 1961 to 2020, annual mean temperature stood at 3.3°C, with a clear north-south temperature gradient emerging across the catchments (Figure 1c), highlighting the variation in temperature distribution within the dataset. These climatic features collectively influence the streamflow generation (Figure 1d), together with spatial variations in topography (Figure 1e), land use (Figure 1f), and soil classes (Figure 1g).

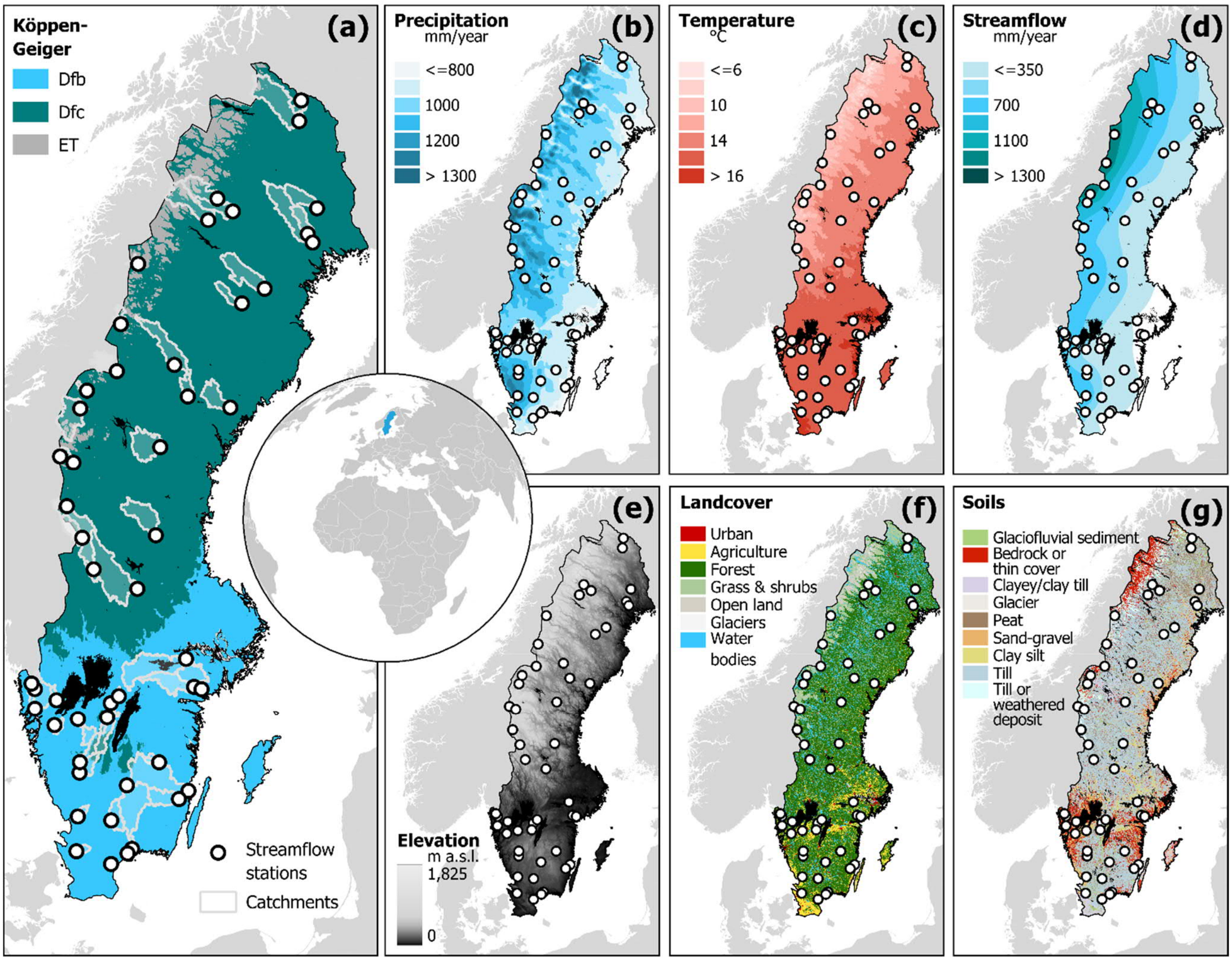

Figure 1: Overview of the 50 streamflow stations and their catchments in relation to Sweden's (a) climate zones according to the Köppen-Geiger classification (Beck et al., 2018)*, including polar tundra climate zone (ET), subarctic boreal climate (Dfc) and warm summer hemiboreal climate (Dfb), (b) mean annual precipitation, (c) mean annual temperature, (d) mean annual streamflow during the period 1961-2020, (e) elevation, (f) land cover classes, and (g) soil classes.*

A pronounced spatial divergence in annual streamflow is also apparent (Figure 1d), with highest runoff rates (810 – 1,312 mm/year) occurring in the Scandinavian Mountains in northwestern Sweden and lowest (168 – 300 mm/year) in Southeastern Sweden. The elevation variability within these catchments is generally relatively low, ranging from 12 to 942 meters above sea level, with mild slopes (Figure 1e). Most of the catchments are covered by forests with limited cultivation, and limited presence of lakes and wetlands (Figure 1f). At the same time, till soils constitute the dominant soil class in 76% of the catchments, followed by bedrock, peat and glaciofluvial sediment (Figure 1g). Roughly one third of the catchments are regulated, but the impact of reservoirs is generally minimal. Glaciers and urban areas are also scarce in these catchments, which is essential for accurate hydrological modeling as simulating runoff from such features poses challenges for many models.

1.2. Data Sources

1.2.1. Streamflow Data

Daily streamflow measurements were sourced from the Swedish Meteorological and Hydrological Institute (SMHI) by accessing their publicly accessible water-related database 'Vattenwebb' (SMHI, 2023a). This platform offered an array of resources, including streamflow maps, observed streamflow data, details about water samples, streamflow regimes, simulated flows for ungauged basins, snow cover information and various other datasets. Notably, the database was exclusively accessible in the Swedish language.

Within this repository, a particular tool called 'Hydrological Observations' hosted data of more than 300 gauging stations, licensed under the Creative Commons Attribution 4.0 International license (CC-BY 4.0). The available data had undergone regular quality checks and has been widely used for hydrological studies in Sweden, hydrological model calibration, national predictions, warnings, and statistical assessments.

From all available stations, only those that had continuous streamflow measurements during the period January 1961 to December 2020 were selected, or those with gaps of up to 14 days, which were then filled through linear interpolation. The streamflow data files provided by SMHI also included information on the gauging station's number (id), name and geographic location (i.e., latitude and longitude in WGS84 projection), catchment area (in km^2), and stream name.

1.2.2. Geospatial Data

To acquire the geospatial data for the streamflow stations and their catchments, the following steps were taken:

- Visualization of a national set of catchments and streams: A polygon shapefile containing more than 55,000 catchment boundaries (with a median area of 3 km^2) and a line shapefile containing more than 135,000 stream segments across Sweden were obtained from SMHI's SVAR database (SMHI, 2023b). The database, available only in Swedish, provided comprehensive information on Swedish lakes, streams and catchments (Eklund, 2011; Henestål et al., 2015). The shapefiles were processed using QGIS, an open-source cross-platform GIS application (*https://qgis.org/*).
- Localization of streamflow stations: In QGIS, a new point shapefile was created to visualize the locations of the streamflow stations based on the latitude and longitude information available in the original streamflow data files. A rigorous quality check was

performed on this point shapefile, following the criteria that each streamflow station should be situated within the water of a stream and at the outlet of a catchment. Specifically, points were assessed for their intersection with stream segments in the line layer and catchment boundaries in the polygon layer. If a point did not meet this condition, it was manually relocated to the nearest stream and catchment boundary. To ensure accuracy, the final locations of all gauging stations were cross-validated against the stream names and locations on digital maps to confirm that the stream and catchment names matched the station information.

- Identification of the upstream catchment area: For each station in the point shapefile, the corresponding catchment boundary was extracted from the polygon file. However, as these relatively small polygons only represented subcatchments that encompassed the respective gauging station, an automated procedure was necessary to obtain the entire upstream area, which typically comprised multiple subcatchments. Since each catchment boundary in the polygon shapefile contained information on the downstream catchment it was draining into, a recursive approach was employed. Beginning from the outlet, all upstream catchments that contributed to this particular subcatchment were systematically traced (Figure 2). This process was then repeated for the identified upstream catchments, progressively reaching further away from the catchment outlet, until no further upstream catchments could be detected. Through this procedure, the complete upstream catchment area for each streamflow station could be successfully obtained by merging all the identified subcatchments into one polygon feature. The resulting shapefiles are included in the provided dataset.

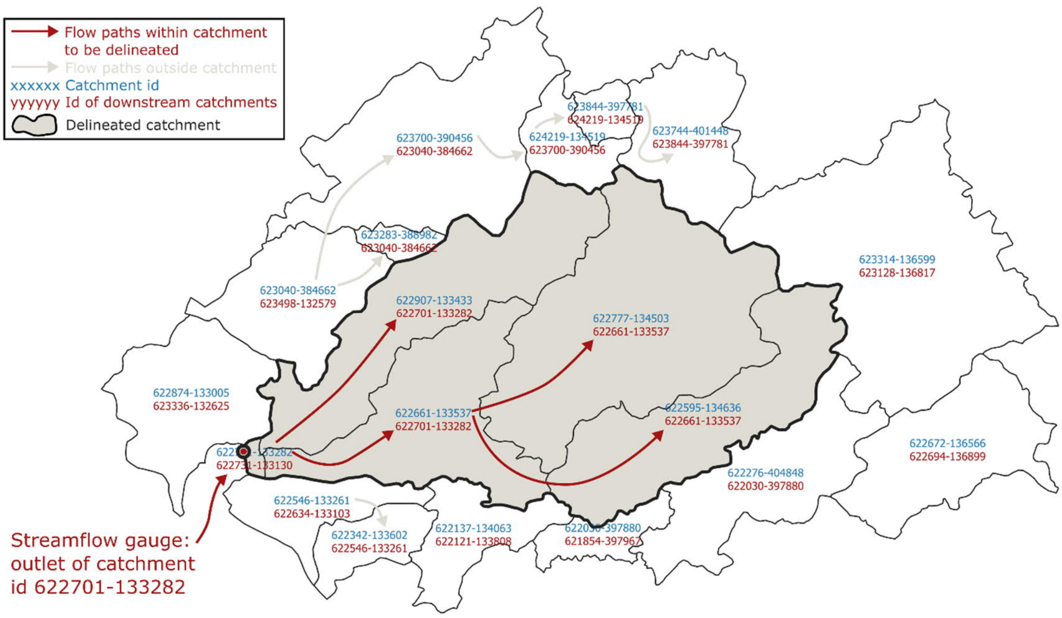

Figure 2: Exemplified procedure of tracing the upstream contributing catchment areas.

1.2.3. Catchment Properties

Computations of catchment properties, including area, mean elevation, slope, landcover, climate zones, soil classes and human activities (i.e., river regulation) were carried out using QGIS with the aid of shape and raster files. Mean elevation and slope metrics for each catchment were calculated based on the European Digital Elevation Model (EU-DEM) version 1.1, a raster layer with a resolution of 25m x 25m provided by the European Environment Agency (EEA, 2023a).

The distribution of landcover categories for each catchment were deduced from the raster-based Corine Land Cover (CLC) 2018 dataset, Version 2020-20u1 (Büttner, 2014; EEA, 2023b). The 28 distinct landcover classes within the Swedish catchments were aggregated into eight broader parent classes: urban, agriculture, forest, grassland and shrubs, open land, glaciers, wetlands as well as water bodies (i.e., lakes and streams). To compute the percentage of each class within a given catchment, the number of grid cells corresponding to each class present within the catchment boundaries was analyzed.

The dataset also incorporates catchment-wise information concerning the Köppen-Geiger climate zone, derived from a raster layer developed by Beck et al. (2018), available under a CC BY 4.0 license (GloH2O, 2021). Insights into soil classes were sourced from the Swedish Geological Survey (SGU) through their publicly available Swedish national soil type database (SGU, 2023), exclusively accessible in the Swedish language. It is important to note that this database was geographically confined to the Swedish border, thus constraining its applicability to the small number of transboundary catchments included in the dataset (Figure 3a). This is particularly relevant for two catchments where the outlet is situated in Sweden, but 98% (Figure 3b) respective 55% (Figure 3c) of their catchment area stretches into Norway.

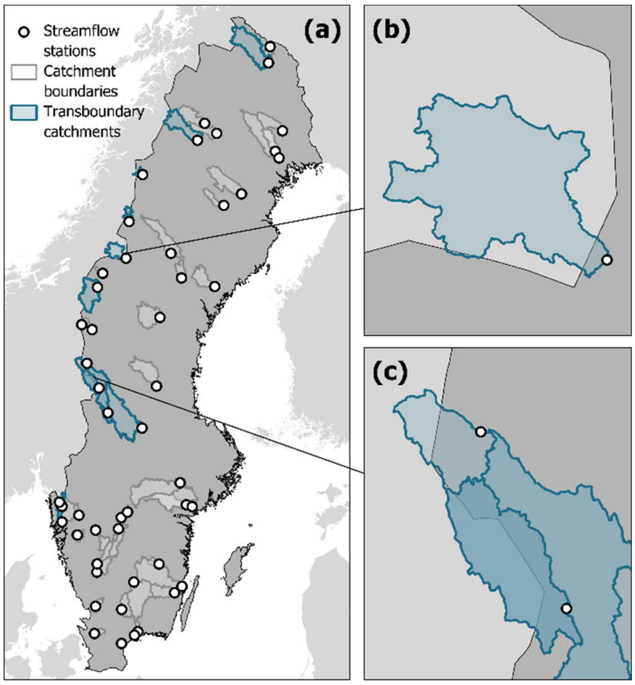

Figure 3: Practical issues when extracting soil data for transboundary catchments from a national source.

Degree of regulation (DOR), representing reservoir volume relative to the mean annual flow volume from its draining area, alongside regulated volume were also extracted from SMHI's 'Vattenwebb' database (SMHI, 2023a). However, it is important to note that this information was not directly linked to the hydrological observations (see 1.2.1 Streamflow Data). Instead, this information was concealed in a separate tool called 'Modelled Data by Catchment Area', which supplied modeled streamflow data for each of the nearly 55,000 catchments in Sweden, which have been simulated with the national S-HYPE model (Strömqvist et al., 2012; Bergstrand, 2014; Girons Lopez et al., 2021). To ensure a comprehensive and integrated dataset, this information had to be manually linked to the streamflow observations presented in this study.

1.2.4. Catchment Selection Criteria

Drawing upon the streamflow data and extracted catchment properties, a careful selection of catchments was made, adhering to specific criteria to guarantee data quality and suitability for diverse analyses:

- Only catchments unaffected by bifurcations or backwater effects were included.
- Consideration was limited to catchments with low percentages (<5%) of glaciers and urbanized areas.
- Catchments with low DOR (<20%) were exclusively chosen.

In total, 50 catchments fulfilled all the specified criteria (Figure 1a). Notably, six of these catchments were nested within larger catchments.

1.2.5. Meteorological Data

Gridded daily mean temperature and precipitation data for each of these 50 catchments were obtained from SMHI's openly available PTHBV database (SMHI, 2023c). This platform with a Swedish interface provided spatially interpolated 4 km x 4 km national grids for the period 1961-2020, which are commonly used by SMHI for computations with the national hydrological models S-HYPE (Strömqvist et al., 2012; Bergstrand, 2014; Girons Lopez et al., 2021) and HBV (Bergström, 1992; Seibert and Vis, 2012). The data was available in the nedcdf file format, which was processed in the scientific programming and numeric computing platform MATLAB (www.mathworks.com). Catchment-specific temperature and precipitation values were calculated through an area-weighted average of all grid cells partly or fully lying within the catchment boundaries.

1.2.6. Hydrological Signatures

Hydrological signatures are a powerful tool to characterize catchment-specific dynamic functioning and hydrological responses (Wagener et al., 2007; Yadav et al., 2007; Gupta et al., 2008; Toth, 2013). A broad spectrum of potential streamflow signatures have been employed in the scientific literature (Clausen and Biggs, 2000; Shamir et al., 2005; Yadav et al., 2007; Ley et al., 2011), e.g., for testing and improving hydrological models (Yilmaz et al., 2008), in ecological studies (Pool et al., 2017) and for evaluating model performance under non-stationary conditions (Stahl et al., 2011; Mendoza et al., 2015). To depict the (1) comprehensive water balance and runoff dynamics, (2) seasonal dynamics, (3) low flow, and (4) high flow conditions, a collection of 16 distinct hydrological signatures (Table 2) was computed following the selection by Tootoonchi et al. (2022, 2023). These signatures could be easily derived from the available observed precipitation and streamflow data. Most if these signatures were computed on an annual basis, and thereafter averaged over the entire record period. The dataset includes three values of each signature: (1) an average value for CNP 1 (1961-1990), an average value for CNP 2 (1991-2020) and (3) an average value over the entire record period (1961-2020).

Table 2: Overview and description of hydrological signatures provided in the dataset

Category	No	Hydrological signatures (abbreviation)	Description	Reference
Water balance and flow dynamics	S01	Mean annual flow, (Qmean)	Average flow in a year (mm year^{-1}).	(Yilmaz et al., 2008)
	S02	Runoff coefficient, (Qcoeff)	Fraction of the total yearly precipitation that generates flow: $Q_{coeff} = \frac{\sum_i Q_i}{\sum_i P_i}$, Where Q_i represents the daily flow (in mm·day^{-1}) and P_i, daily precipitation, both of which were summed over a year.	(Yadav et al., 2007)
	S03	Timing of the center of mass of annual flow, (COM)	Timing is computed from daily flows Q_i and for each year: $COM = \frac{\sum_i Q_i t_i}{\sum_i Q_i}$ where t_i represents ordinal day of a year.	(Mendoza et al., 2015)
	S04	Spring onset (spring "pulse day"), (SPD)	Spring onset is the ordinal number of the day in which the negative difference between the streamflow mass curve and the mean streamflow mass curve is the greatest. Spring onset series is obtained from values in each year	(Cunderlik and Ouarda, 2009)
Seasonal flow dynamics	S05	Mean spring flow, (Qmean_spring)	Flows in the spring (1st March through 31st May) in each year.	(Teutschbein et al., 2015, 2018)
	S06	Mean summer flow, (Qmean_summer)	Flows in the summer (1st June through 31st August) in each year.	
	S07	Mean autumn flow, (Qmean_autumn)	Flows in the autumn (1st September through 30st November) in each year.	
	S08	Mean winter flow, (Qmean_winter)	Flows in the winter (1st December through 28th February) in each year.	
Low flow characteristics	S09	Low-flow frequency, (LFfreq)	Number of days in a year with flows lower than the 20th percentile of all flow values in the full record period	(Krysanova et al., 2017)
	S010	Timing of 30-day low flow, (T_minQ_d30)	Ordinal day in which 15th day of the 30-day minimum annual flow occurred, obtained in each year. If there were several consecutive days with the same minimum flows, the mean timing of these days in a year is adopted.	(Richter et al., 1998; Sadri et al., 2016)
	S011	7-day low flow, (minQ_d7)	Minimum flows averaged over a given number of consecutive days (here, 7 and 30) obtained in each year.	(Comer and Zimmermann, 1968; Richter et al., 1998; Khaliq et al., 2008)
	S012	30-day low flow, (minQ_d30)		
high flow characteristics	S013	High flow frequency, (HFfreq)	Number of days in a year with flows higher than the 80th percentile of all flow values in the full record period	(Krysanova et al., 2017)
	S014	Timing of the 1-day high flow, (T_maxQ_d1)	Ordinal day in which the maximum annual flow occurred, obtained in each year of the observed period.	(Richter et al., 1998)
	S015	30-day high flow, (maxQ_d30)	Maximum flows averaged over a given number of days (here, 30 and 1) obtained in each year.	(Richter et al., 1998)
	S016	1-day high flow, (maxQ_d1)		

2. Dataset Access

This dataset exclusively consists of shape (.shp) and comma-delimited text (.csv) files that were compressed into .zip files. All file formats are easily viewable and modifiable using freely available software such as 7zip, QGIS or R. The dataset has been structured into three main directories (each compressed into a separate .zip file) to ensure systematic organization:

1. Catchment GIS shapefiles: This directory contains two distinct shapefiles in EPSG:4326 - WGS 84 projection. One outlines the boundaries of each catchment in polygon format, the other marks the corresponding outlets, representing streamflow stations.

2. Catchment time series: Within this directory, individual files for each of the 50 catchments can be found. These files contain the measured daily hydroclimatic variables. Further details about the abbreviations and variables used in these files can be found in Table 3.

3. Catchment properties: This directory includes separate files for the physical catchment properties, land cover data, soil classifications, and hydrological signatures. Each of these files consolidates information related to all 50 catchments.

    3.1. Physical catchment properties: Offers insights into the geographical location and physical attributes of each catchment. Abbreviations and variables are elaborated upon in Table 3.

    3.2. Landcover: Encompasses data on eight distinct land cover classes, along with their proportional distribution within each catchment. Table 4 provides further details about the relevant abbreviations and variables.

    3.3. Soil classes: Provides information about ten discrete soil categories and their respective distribution within each catchment. Refer Table 4 to for clarification on abbreviations and variables.

    3.4. Hydrological signatures: These are divided into three separate files, one covering the entire record period (1961-2020), another for the CNP1 (1961-1990), and a third for the CNP2 (1991-2020). It's important to note that the mean streamflow used as reference for computing low- and high-flow frequencies across all three instances was computed from the entire record period (see explanations in Table 2).

Table 3: Content of the observed time series files and physical catchment properties

Category	Variable Name	Description	Unit name	Unit abbr.
Catchment time series	Year	Date identifiers (year, month, day) according to the modern-day Gregorian calendar	-	[-]
	Month		-	[-]
	Day		-	[-]
	Qobs_m3s	Observed daily streamflow values	Cubic meter per second	[m^3/s]
	Qobs_mm	Observed daily streamflow values	Millimetre per day	[mm/day]
	Pobs_mm	Observed daily precipitation values	Millimetre per day	[mm/day]
	Tobs_C	Observed daily temperature values	Degrees Celsius	[°C]
Catchment physical properties	ID	Unique catchment identifier specific for each catchment	-	[-]
	Name	Unique catchment name	-	[-]
	Latitude_WGS84	Latitudinal coordinate of the streamflow station in WGS84 projection	Degrees North	[°N]
	Longitude_WGS84	Longitudinal coordinate of the streamflow station in WGS84 projection	Degrees East	[°E]
	Area_km2	Size of the catchment area contributing to the associated streamflow station	Square kilometre	[km^2]
	Elevation_mabsl	Average catchment elevation	Meters above sea level	[m a.s.l.]
	Slope_mean_degree	Average slope across the catchment	Degrees	[°]
	DOR	Degree of regulation, i.e., reservoir volume relative to the mean annual flow volume from its draining area	Percentage	[%]
	RegVol_m3	Regulated volume	Cubic meter	[m^3]
	Pmean_mm_year	Average annual precipitation over the full record period 1961-2020	Millimetre per year	[mm/yr]
	Tmean_C	Average annual temperature over the full record period 1961-2020	Degrees Celsius	[°C]

Table 4: Overview and explanation of variables in the landcover and soil class files

Category	Variable Name	Description	Unit name	Unit abbr.
Landcover	Urban_percentage	Fraction of urban area, including industrial and commercial units, roas networks, airports, dump sites, construction sites, etc.	Percentage	[%]
	Water_percentage	Fraction of water bodies, including streams and lakes	Percentage	[%]
	Forest_percentage	Fraction of forest cover, comprising broad-leaved, coniferous and mixed forests	Percentage	[%]
	Open_land_percentage	Fraction of open land, inclusive of beaches, bare rocks, sparsely vegetated and burnt areas	Percentage	[%]
	Agriculture_percentage	Fraction of agricultural land, including all types of arable and irrigated land, pastures, agro-forestry areas and all types of fruit plantations	Percentage	[%]
	Glaciers_percentage	Fraction of glaciers and perpetual snow	Percentage	[%]
	Shrubs_and_grassland_percentage	Fraction of shrubs and grasslands, encompassing natural grasslands, moors and heathland, as well as transitional woodland-shrubland, etc.	Percentage	[%]
	Wetlands_percentage	Fraction of wetlands, including inland marshes, peat bogs and salt marshes	Percentage	[%]
Soil class	Glaciofluvial_sediment_percentage	Proportion of glaciofluvial sediments	Percentage	[%]
	Bedrock_percentage	Proportion of bedrock	Percentage	[%]
	Postglacial_sand_and_gravel_percentage	Proportion of postglacial sand and gravel	Percentage	[%]
	Till_percentage	Proportion of till	Percentage	[%]
	Water_percentage	Proportion of water bodies (i.e., streams and lakes)	Percentage	[%]
	Peat_percentage	Proportion of peat soils	Percentage	[%]
	Silt_percentage	Proportion of silt	Percentage	[%]
	Clayey_till_and_clay_till_percentage	Proportion of clayey till and clay till	Percentage	[%]
	Till_and_weathered_deposit_percentage	Proportion of till and weathered deposits	Percentage	[%]
	Glacier_percentage	Proportion of glaciers	Percentage	[%]

3. Acknowledgements

The lead author responsible for the data collection and compilation presented in this paper was funded by the Swedish Research Council For Sustainable Development (FORMAS, grant no. 942-2015-1123), the Swedish Research Council (VR, grant no. 2017-04970), and Uppsala University Department of Earth Sciences, Program for Air, Water and Landscape Sciences.

4. References

Beck HE, Zimmermann NE, McVicar TR, Vergopolan N, Berg A, Wood EF. 2018. Present and future Köppen-Geiger climate classification maps at 1-km resolution. Scientific Data 5 (1): 180214 DOI: 10.1038/sdata.2018.214

Bergstrand M. 2014. Nationwide hydrological statistics for Sweden with high resolution using the hydrological model S-HYPE. Hydrology Research 45 (3): 349–356 DOI: 10.2166/nh.2013.010

Bergström S. 1992. The HBV model - its structure and applications. Swedish Meteorological and Hydrological Institute (SMHI), Norrköping, Sweden. Available at: https://www.smhi.se/polopoly_fs/1.83592!/Menu/general/extGroup/attachmentColHold/mainCol1/file/RH_4.pdf

Büttner G. 2014. CORINE Land Cover and Land Cover Change Products. In Land Use and Land Cover Mapping in Europe: Practices & Trends, Manakos I, , Braun M (eds).Springer Netherlands: Dordrecht; 55–74. DOI: 10.1007/978-94-007-7969-3_5

Clausen B, Biggs BJF. 2000. Flow variables for ecological studies in temperate streams: groupings based on covariance. Journal of Hydrology 237 (3–4): 184–197 DOI: 10.1016/S0022-1694(00)00306-1

Comer GH, Zimmermann RC. 1968. Low-flow and basin characteristics of two streams in Northern Vermont. Journal of Hydrology 7 (1): 98–108 DOI: 10.1016/0022-1694(68)90197-2

Cunderlik JM, Ouarda TBMJ. 2009. Trends in the timing and magnitude of floods in Canada. Journal of Hydrology 375 (3): 471–480 DOI: 10.1016/j.jhydrol.2009.06.050

EEA. 2023a. European Digital Elevation Model (EU-DEM), version 1.1. Copernicus Land Monitoring Service, European Environment Agency Available at: https://land.copernicus.eu/imagery-in-situ/eu-dem/eu-dem-v1.1 [Accessed 10 August 2023]

EEA. 2023b. Corine Land Cover (CLC) 2018, Version 2020_20u1. Copernicus Land Monitoring Service, European Environment Agency Available at: https://land.copernicus.eu/pan-european/corine-land-cover/clc2018 [Accessed 10 August 2023]

Eklund A. 2011. SVAR, Svenskt vattenarkiv. 53. Swedish Meteorological and Hydrological Institute (SMHI), Norrköping, Sweden. Available at: https://www.smhi.se/polopoly_fs/1.17832!/webbFaktablad_53.pdf

Girons Lopez M, Crochemore L, G. Pechlivanidis I. 2021. Benchmarking an operational hydrological model for providing seasonal forecasts in Sweden. Hydrology and Earth System Sciences 25 (3): 1189–1209 DOI: 10.5194/hess-25-1189-2021

GloH2O. 2021. Köppen-Geiger: Global 1-km climate classification maps. https://www.gloh2o.org Available at: https://www.gloh2o.org/koppen/ [Accessed 10 August 2023]

Gupta HV, Wagener T, Liu Y. 2008. Reconciling theory with observations: elements of a diagnostic approach to model evaluation. Hydrological Processes 22 (18): 3802–3813 DOI: 10.1002/hyp.6989

Henestål J, Ranung J, Gyllander A, Johnson Å, Olsson H, Pettersson O, Westman Y, Wingqvist E-M. 2015. Arbete med SVAR version 2012_1 och 2012_2, Svenskt Vattenarkiv, en databas vid SMHI [Work with SVAR version 2012_1 and 2012_2, Swedish Water Archive, a database at SMH]. Swedish Meteorological and Hydrological Institute (SMHI), Norrköping, Sweden.

Khaliq MN, Ouarda TBMJ, Gachon P, Sushama L. 2008. Temporal evolution of low-flow regimes in Canadian rivers. Water Resources Research 44 (8) DOI: 10.1029/2007WR006132

Krysanova V, Vetter T, Eisner S, Huang S, Pechlivanidis I, Strauch M, Gelfan A, Kumar R, Aich V, Arheimer B, et al. 2017. Intercomparison of regional-scale hydrological models and climate change impacts projected for 12 large river basins worldwide—a synthesis. Environmental Research Letters 12 (10): 105002 DOI: 10.1088/1748-9326/aa8359

Ley R, Casper MC, Hellebrand H, Merz R. 2011. Catchment classification by runoff behaviour with self-organizing maps (SOM). Hydrology and Earth System Sciences 15 (9): 2947–2962 DOI: 10.5194/hess-15-2947-2011

Mendoza PA, Clark MP, Mizukami N, Newman AJ, Barlage M, Gutmann ED, Rasmussen RM, Rajagopalan B, Brekke LD, Arnold JR. 2015. Effects of Hydrologic Model Choice and Calibration on the Portrayal of Climate Change Impacts. Journal of Hydrometeorology 16 (2): 762–780 DOI: 10.1175/JHM-D-14-0104.1

Pool S, Vis MJP, Knight RR, Seibert J. 2017. Streamflow characteristics from modeled runoff time series – importance of calibration criteria selection. Hydrology and Earth System Sciences 21 (11): 5443–5457 DOI: 10.5194/hess-21-5443-2017

Richter BD, Baumgartner JV, Braun DP, Powell J. 1998. A spatial assessment of hydrologic alteration within a river network. Regulated Rivers: Research & Management 14 (4): 329–340 DOI: 10.1002/(SICI)1099-1646(199807/08)14:4<329::AID-RRR505>3.0.CO;2-E

Sadri S, Kam J, Sheffield J. 2016. Nonstationarity of low flows and their timing in the eastern United States. Hydrology and Earth System Sciences 20 (2): 633–649 DOI: 10.5194/hess-20-633-2016

Seibert J, Vis MJP. 2012. Teaching hydrological modeling with a user-friendly catchment-runoff-model software package. Hydrology and Earth System Sciences 16 (9): 3315–3325 DOI: 10.5194/hess-16-3315-2012

SGU. 2023. Jordarter 1:1 miljon [en: Soil types 1:1 million]. Jordartsdata [en: Soil data] Available at: https://www.sgu.se/produkter-och-tjanster/geologiska-data/vara-data-per-amnesomrade/jordartsdata/jordarter-11-miljon/ [Accessed 10 August 2023]

Shamir E, Imam B, Gupta HV, Sorooshian S. 2005. Application of temporal streamflow descriptors in hydrologic model parameter estimation. Water Resources Research 41 (6): W06021 DOI: 10.1029/2004WR003409

SMHI. 2023a. Vattenwebb [en: Water Web]. Vattenwebb | SMHI Available at: https://www.smhi.se/data/hydrologi/vattenwebb [Accessed 10 August 2023]

SMHI. 2023b. SVAR - Svenskt Vattenarkiv [en: Swedish Water Archive]. Ladda ner data från Svenskt Vattenarkiv [en: Download data from the Swedish Water Archive] Available at: https://www.smhi.se/data/hydrologi/sjoar-och-vattendrag/ladda-ner-data-fran-svenskt-vattenarkiv-1.20127 [Accessed 10 August 2023]

SMHI. 2023c. Nedladdning av griddad nederbörd- och temperaturdata [en: Download of gridded precipitation and temperature data]. PTHBV Available at: https://www.smhi.se/data/ladda-ner-data/griddade-nederbord-och-temperaturdata-pthbv [Accessed 10 August 2023]

Stahl K, Tallaksen LM, Gudmundsson L, Christensen JH. 2011. Streamflow Data from Small Basins: A Challenging Test to High-Resolution Regional Climate Modeling. Journal of Hydrometeorology 12 (5): 900–912 DOI: 10.1175/2011JHM1356.1

Strömqvist J, Arheimer B, Dahné J, Donnelly C, Lindström G. 2012. Water and nutrient predictions in ungauged basins: set-up and evaluation of a model at the national scale. Hydrological Sciences Journal 57 (2): 229–247 DOI: 10.1080/02626667.2011.637497

Teutschbein C, Grabs T, Karlsen RH, Laudon H, Bishop K. 2015. Hydrological response to changing climate conditions: Spatial streamflow variability in the boreal region. Water Resources Research 51 (12): 9425–9446 DOI: 10.1002/2015WR017337

Teutschbein C, Grabs T, Laudon H, Karlsen RH, Bishop K. 2018. Simulating streamflow in ungauged basins under a changing climate: The importance of landscape characteristics. Journal of Hydrology 561: 160–178 DOI: 10.1016/j.jhydrol.2018.03.060

Tootoonchi F, Haerter JO, Todorović A, Räty O, Grabs T, Teutschbein C. 2022. Uni- and multivariate bias adjustment methods in Nordic catchments: Complexity and performance in a changing climate. Science of The Total Environment 853: 158615 DOI: 10.1016/j.scitotenv.2022.158615

Tootoonchi F, Todorović A, Grabs T, Teutschbein C. 2023. Uni- and multivariate bias adjustment of climate model simulations in Nordic catchments: Effects on hydrological signatures relevant for water resources management in a changing climate. Journal of Hydrology 623: 129807 DOI: 10.1016/j.jhydrol.2023.129807

Toth E. 2013. Catchment classification based on characterisation of streamflow and precipitation time series. Hydrology and Earth System Sciences 17 (3): 1149–1159 DOI: 10.5194/hess-17-1149-2013

Wagener T, Sivapalan M, Troch P, Woods R. 2007. Catchment Classification and Hydrologic Similarity. Geography Compass 1 (4): 901–931 DOI: 10.1111/j.1749-8198.2007.00039.x

Yadav M, Wagener T, Gupta H. 2007. Regionalization of constraints on expected watershed response behavior for improved predictions in ungauged basins. Advances in Water Resources 30 (8): 1756–1774 DOI: 10.1016/j.advwatres.2007.01.005

Yilmaz KK, Gupta HV, Wagener T. 2008. A process-based diagnostic approach to model evaluation: Application to the NWS distributed hydrologic model. Water Resources Research 44 (9): W09417 DOI: 10.1029/2007WR006716